Report

TST08-09-10-R v1

Report for the ICRS Trainings on Biomechanics

Testing Services

Document History

Version	Modification	Effective Date
1	Creation	28 JUN 2011

Review and Approval

Authors of Version:		28 Jun 2011
	Name: Antoine Larouche Title: Director Market Development & Products Specialist	Date: dd mmm yyyy
		28 JUN 2011
	Name: Alexandre Cormier-Belley Title: Intern	Date: dd mmm yyyy
		28 JUN 2011
	Name: Sotcheadt Sim Title: Intern	Date: dd mmm yyyy
Approval:		28 Jun 2011
	Name: Martin Garon Title: President	Date: dd mmm yyyy
		28 JUN 2011
	Name: Éric Quenneville Title: CEO & Quality Assurance	Date: dd mmm yyyy

TABLE OF CONTENTS

1. Abstract

This report presents the results from the three modules of the ICRS training on articular cartilage biomechanics. First, the Arthro-BST's Quantitative Parameter (QP) was mapped *in vitro* over articular cartilage surfaces of 3 to 5 years old female bovine stifle joints. The partial mappings performed by all teams showed excellent correspondences with the reference mappings. Effect of an induced physical defect (hand-held impactor) on lower and higher QP regions was also evaluated based upon the QP before and after the impact delivery. A significant decrease in QP was observed after impact for higher QP regions, while no statistically significant variation was observed for the lower QP regions. Then, indentation tests were performed to obtain a mechanical property of articular cartilage, namely the shear modulus. Those results were compared to the QP acquired with the Arthro-BST. The shear modulus was shown to vary proportionally with the QP previously obtained with the Arthro-BST, supporting that the QP reflects the mechanical properties of cartilages. Finally, unconfined compression tests on articular cartilage discs were performed to obtain other mechanical properties of cartilage, namely the fibril and equilibrium moduli as well as the permeability. An analysis of the results for two compression ramps shows how each parameter changes following compression.

2. Purpose, background & experimental design

Refer to the protocols **TST08-P v1 Training for Mapping of Articular Cartilage Surfaces in Large Animals Using the Arthro-BST**, **TST09-P v1 Training for Indentation of Articular Cartilage in Large Animals Using the Mach-1** and **TST10-P v1 Training for Unconfined Compression of Articular Cartilage in Large Animals Using the Mach-1** in Appendix I.

3. Definitions & acronyms

QP	Quantitative Parameter

4. Team members

Team #	Team members	Sample	Team #	Team members	Sample
1	[redacted]	Right tibial plateau	7	[redacted]	Left tibial plateau
2		Right femoral condyles	8		Left femoral condyles
3		Right trochlea	9		Left trochlea
4		Right tibial plateau	10		Left tibial plateau
5		Right femoral condyles	11		Left femoral condyles
6		Right trochlea	12		Left trochlea

5. Results and discussion

The results for all three trainings, *i.e.* mapping the QP using the Arthro-BST, indentation and unconfined compression of articular cartilage using the Mach-1, are presented in the following sections. Raw data and results are in Appendix II.

5.1 TST08 - Mapping of articular cartilage surfaces in large animals using the Arthro-BST

Mapping of the Quantitative Parameter (QP) was performed using the Arthro-BST on either, the medial and lateral femoral condyles, the trochlea or the tibial plateau of a bovine stifle joint. Each team had to visually assess the general condition of their sample prior to mapping. Table 1 reports all observations for the 12 teams. The observations are ordered by sample types and reflect localized regions on the cartilage surface are identified on sketches (not shown) when applicable.

Table 1 - Observations of articular cartilage surfaces

Team #	Sample types	Observations
1	Tibial plateau	No visual defect
4		Fibrillation & whiter region
7		Fibrillation & thinned on the edges
10		Fibrillation & defect on lateral side
2	Femoral condyle	No visual defect
5		No visual defect
9		Fibrillation on lateral condyle & medial is pinker than lateral condyle
11		Fibrillation on lateral condyle & defect on medial condyle
3	Trochlea	Slight discoloration on medial side
6		Slight discoloration on medial side
9		Fibrillation on lateral side
12		N/A

The samples were held in place in a testing chamber. A digital camera was mounted on a camera stand and "Arthro-BST (Cartilage Mapping)" software was used to load positioning references on the sample surface from a standardized grid.

Following data acquisition, a color-scale overlay representing the results was superimposed on a picture of the cartilage surface. Figure 1 presents the QP mappings obtained by all teams as well as a reference QP mapping for each surface to show the common patterns in the stifle joints.

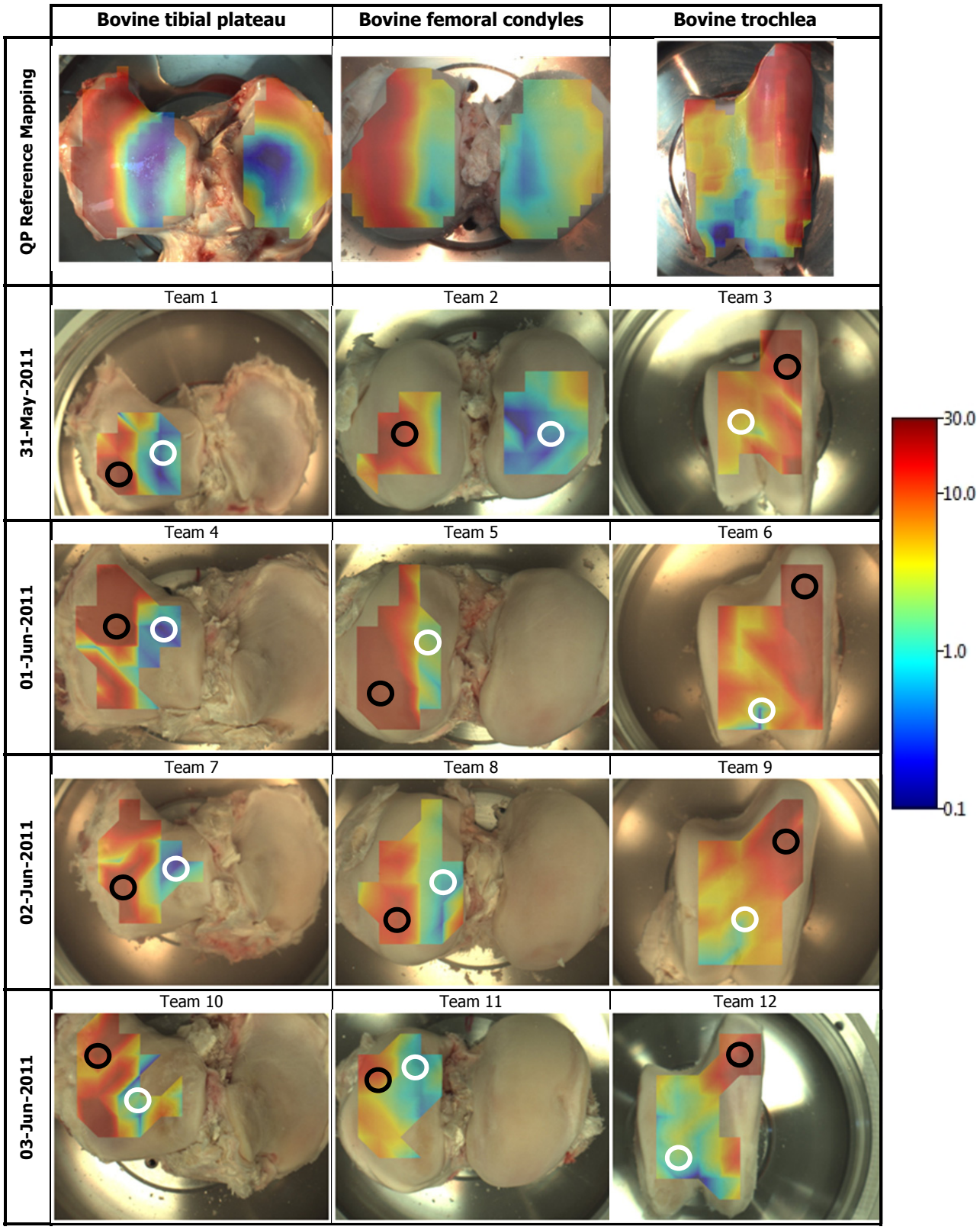

Figure 1 - QP interpolated maps of joints surface (plateau, condyles and trochlea)

Due to the complexity of matching images, no strict statistical analysis of the topographical correlation between the partial mappings generated by all teams and the reference mappings was performed. However, similarities in the QP distributions can be qualitatively observed for all teams. Also, all partial mappings performed matched the reference values and their spatial distribution. These results support the user independence and reproducibility claims of the device.

To assess the effect of a cartilage defect on the QP, controlled defects were generated using a custom-built hand-held impactor on the cartilage surface. The defects were created on regions identified as having higher QP (black circles on Figure 1) and lower QP (white circles on Figure 1). New measurements were performed on the areas around the defects. Figure 2 shows the average QP before and after impact for the regions with higher and lower QP.

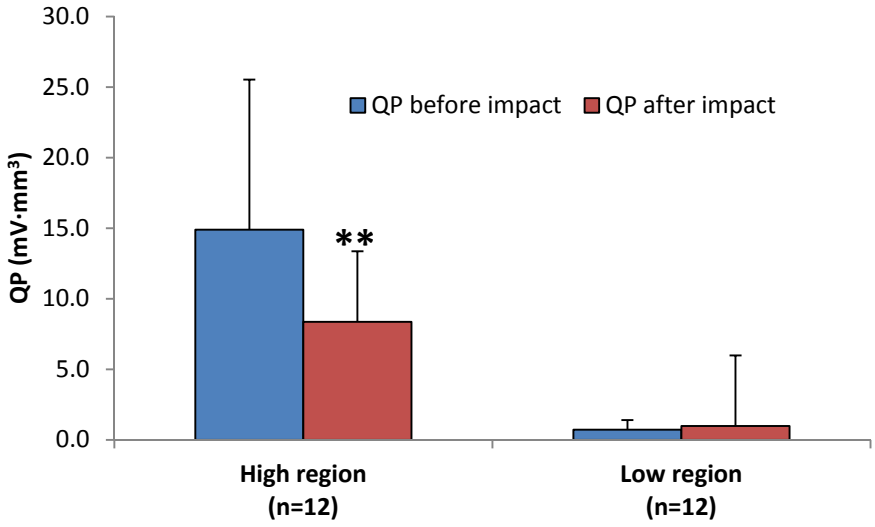

Figure 2 - QP value before and after impact delivery in high and low QP regions.

A paired Student's *t*-test was performed to assess whether the differences between the QP before and after impact are significant. Significant differences were obtained between before and after impact for the high QP regions ($p < 0.01$; indicated by the stars (**) on Figure 2) with an average decrease in QP of 37%. No significant differences were however obtained between before and after impact for the low QP regions ($p > 0.05$).

5.2 TST09 Indentation of Articular Cartilage in Large Animals Using the Mach-1

Osteochondral blocks were cut from either, the medial and lateral femoral condyles, the trochlea, or the tibial plateau of a bovine stifle joint. Indentations were then performed on regions identified as having higher and lower QP as measured with the Arthro-BST. The thickness of articular cartilage on each block was then assessed with a needle technique. Result analyses were performed using Mach-1 Analysis software that considers the indentation mechanics of an infinite elastic layer bonded to a rigid half-space as a model for the layered geometry of cartilage and subchondral bone. The average resulting shear moduli of the cartilage for the higher and lower QP regions are presented in Figure 3.

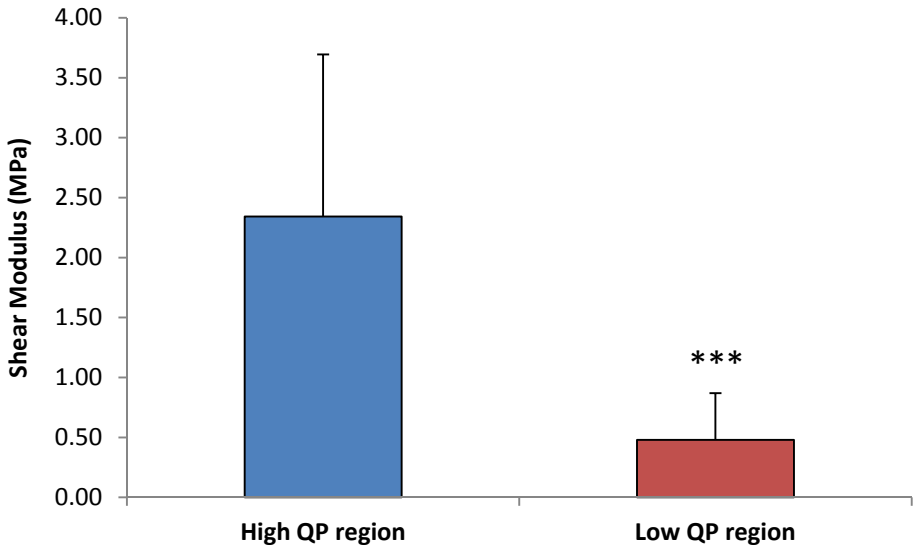

Figure 3 – Average shear moduli for high and low QP regions

A paired Student's *t*-test was performed to assess whether the differences between the shear moduli of higher and lower QP regions are significant. A very significant difference was obtained ($p < 0.001$ indicated by the stars (***) on Figure 3) with an average decrease in QP of 80%.

As presented in Garon *et al.* (2007), the shear modulus is directly proportional to the QP. Plotting the resulting data yield the graph from Figure 4. A linear fit gives a R^2 factor of 0.74.

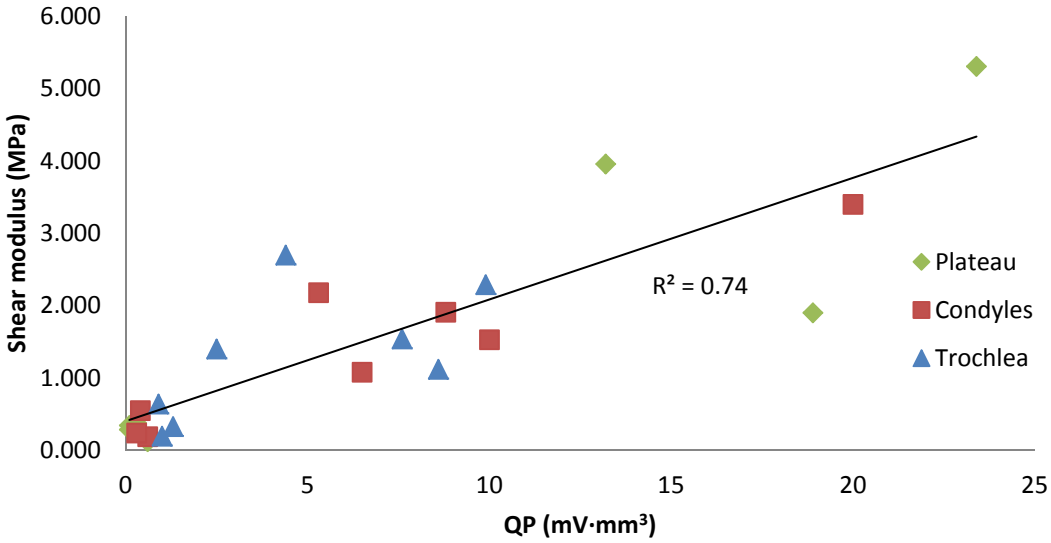

Figure 4 - Shear modulus vs. QP

Note that the important dispersions observed in the calculated moduli for each region can be mainly ascribed to the variability in the cartilage tested (e.g. different animals and different locations in different joints).

5.3 TST10 Unconfined Compression of Articular Cartilage in Large Animals Using the Mach-1

Cartilage discs were extracted from either, the medial and lateral femoral condyles, the trochlea or the tibial plateau of a bovine stifle joint. The thickness of articular cartilage on each disc was first assessed under a dissection microscope and then using the "Find Contact" function of the Mach-1. Figure 5 show the maximum and the average cartilage thicknesses measured under the microscope plotted against the thickness as measured with the Mach-1.

Fitting the two sets of results tends to indicate that, with the parameters for the "Find Contact" function used in this test, the Mach-1 gives a better evaluation of the maximum thickness of the sample than of the average thickness: the thickness measured by the Mach-1 corresponds to 1.05 times the maximum thickness and 1.18 times the average thickness. This is a good reminder that the samples are not perfect discs and that the top cartilage surface is not necessarily flat and parallel to the bottom bone surface.

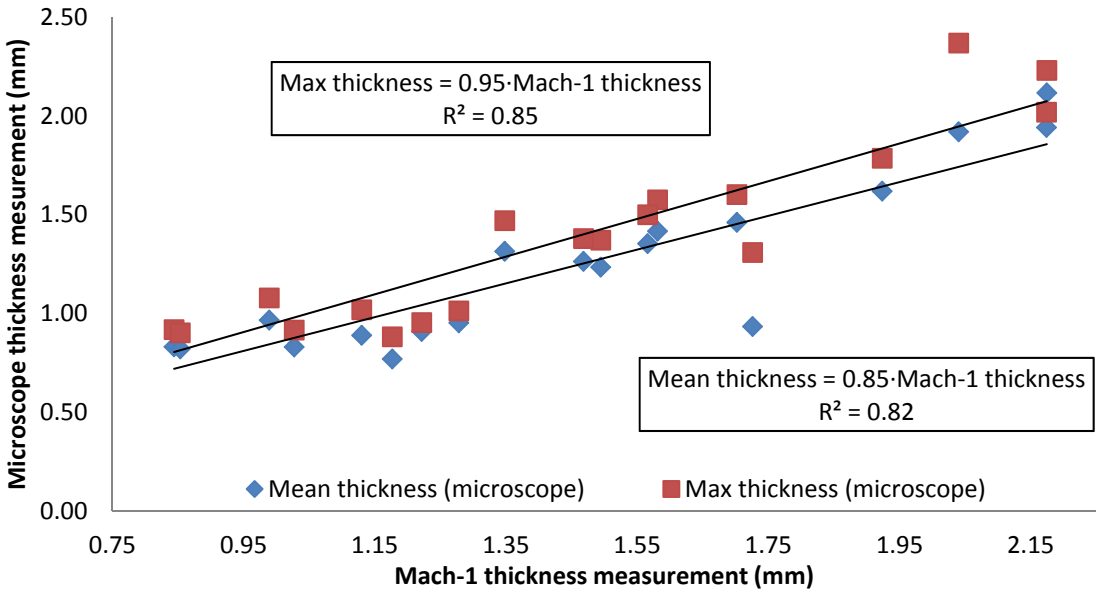

Figure 5 - Maximum and average cartilage thicknesses measured under the microscope vs. cartilage thickness measured with the Mach-1

The discs were finally tested under unconfined compression and the results fitted to the linear fibril-network-reinforced biphasic model (Soulhat *et al.* 1999) to obtain their mechanical properties. Figure 6 shows the average results for (A) the fibril modulus, (B) the equilibrium modulus and (C) the permeability parameter.

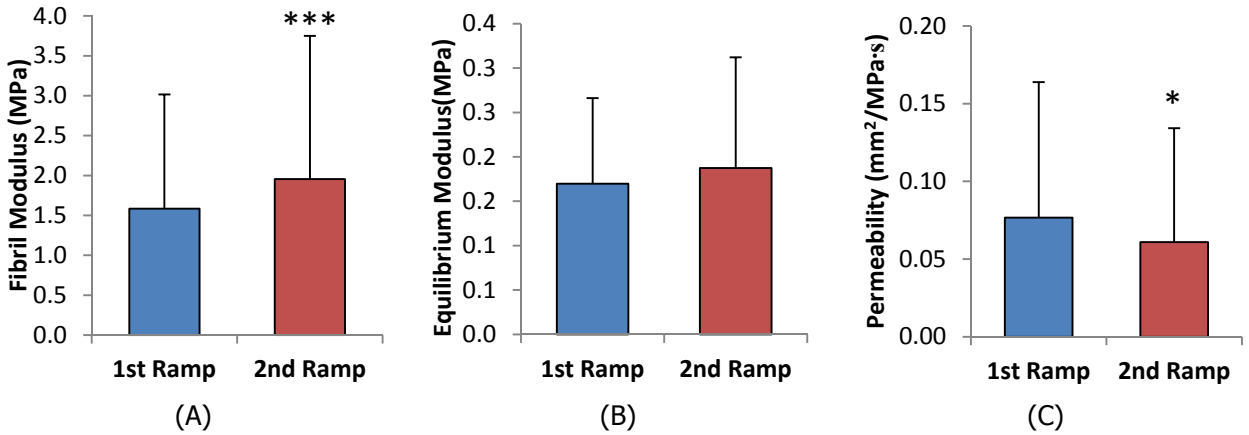

Figure 6 – Average (A) fibril moduli, (B) equilibrium moduli and (C) the permeabilities for the 2 ramps of the unconfined compression test

Paired Student's *t*-tests were performed to assess whether the difference between the mechanical properties obtained for the first and second ramp were significantly different. The difference between the fibril moduli of the first and the second ramp is found to be very significant ($p < 0.001$), with the modulus being greater for the second ramp than for the first. This follows the expected behaviour as the more articular cartilage is compressed, the more the collagen fibrils aligned themselves and yield a greater tensile force. The difference between the equilibrium moduli was found to be not significant ($p > 0.05$). This again was to be expected as this parameter reflects the mechanical property of the matrix at equilibrium. Finally, the difference between the permeabilities was found to be significant ($p < 0.01$), with the permeability being lower for the second ramp than for the first. This also was expected as compressing articular cartilage reduces the size of the pores, making it harder for fluid to flow in the matrix, hence the lower permeability.

Note that the important dispersions observed in the calculated parameters for each ramp can be mainly ascribed to the variability in the cartilage disks tested (e.g. different animals and different locations in different joints).

6. Conclusion

This report presented the results from the three modules of the ICRS training on articular cartilage biomechanics. First, the partial mappings performed by all teams showed excellent correspondences with the reference mappings. Effect of an induced physical defect (hand-held impactor) on lower and higher QP regions was also evaluated based upon the QP before and after the impact delivery. A significant decrease in QP was observed after impact for higher QP regions, while no statistically significant variation was observed for the lower QP regions. Then, indentation tests were performed to obtain a mechanical property of articular cartilage, namely the shear modulus. The shear modulus was shown to vary proportionally with the QP previously obtained with the Arthro-BST, supporting that the QP reflects the mechanical properties of cartilages. Finally, unconfined compression tests on articular cartilage discs were performed to obtain other mechanical properties of cartilage, namely the fibril and equilibrium moduli as well as the permeability. An analysis of the results for two compression ramps shows how each parameter changes following compression.

7. References

Changoor, A. (2011) *Electromechanical and polarization microscopy evaluation of cartilage repair and degeneration*. Présentée à l'Université de Montréal en vue de l'obtention du diplôme de Ph.D. en génie biomédical.

Changoor, A., Fereydoonzad, L., Yaroshinsky, A., M.B. Buschmann, M.D. (2010). *Effects of Refrigeration and Freezing on the Electromechanical and Biomechanical Properties of Articular Cartilage.* ASME J. Biomech. Eng., 132, in press.

Changoor, A., Quenneville, E., Garon, M., Hurtig, M.B., Buschmann M.D. (2009). *Streaming potential-based arthroscopic device can detect changes immediately following localized impact in an equine impact model of osteoarthritis*. Osteoarthritis and Cartilage, Vol. 17, Supplement 1, S53, World Congress on Osteoarthritis, September 2009, Montreal, Quebec, Canada.

Changoor, A., Quenneville, E., Garon, M., Cloutier, L., Hurtig, M.B. Buschmann, M.D. (2007). *Streaming potential based arthroscopic instrument discerns topographical differences in cartilage covered and uncovered by meniscus in ovine stifle joints.* Poster presented at the 53rd annual meeting of the Orthopeadic Research Society, San Diego, California.

Frank EH, Grodzinsky AJ, Koob TJ, Eyre DR. (1987) *Streaming potentials: A sensitive index of enzymatic degradation in articular cartilage*. J Orthop Res, 5, pp. 497–508.

Garon, M. (2007) *Conception et validation d'une sonde arthroscopique pour l'évaluation des propriétés électromécaniques fonctionnelles du cartilage articulaire*. Présentée à l'Université de Montréal en vue de l'obtention du diplôme de Ph.D. en génie biomédical.

Garon, M., Cloutier, L. Légaré, A., Quenneville, E. Shive, M. Buschmann, M.D. (2007). *Reliability and correlation to human articular cartilage mechanical properties of a streaming potential based arthroscopic instrument.* Poster presented at the 53rd annual meeting of the Orthopeadic Research Society, San Diego, California.

Hayes, W. C., Keer, L. M., Herrmann, G. et Mockros, L. F. (1972). *A mathematical analysis for indentation tests of articular cartilage*. J Biomech. 5(5): 541-51.

Légaré, A., Garon, M., Guardo, R., Savard P., Poole, A.R., Buschmann, M.D. (2002) *Detection and analysis of cartilage degeneration by spatially resolved streaming potentials*. J Orthop Res, 20, pp. 819–826.

Quenneville, E. (2006) *Les distributions de potentiel électrique dans le cartilage articulaire*. Présentée à l'Université de Montréal en vue de l'obtention du diplôme de Ph.D. en génie biomédical.

Soulhat, J., Buschmann, M. D. and Shirazi-Adl, A. (1999). *Fibril-network-reinforced biphasic model of cartilage in unconfined compression*. Journal of Biomechanical Engineering, Transactions of the ASME. 121(3): 340-347.

8. Appendix List

- Appendix I. Copy of protocols **TST08-P v1 Training for Mapping of Articular Cartilage Surfaces in Large Animals Using the Arthro-BST**, **TST09-P v1 Training for Indentation of Articular Cartilage in Large Animals Using the Mach-1** and **TST10-P v1 Training for Unconfined Compression of Articular Cartilage in Large Animals Using the Mach-1**.
- Appendix II. Raw data and results